

Article

A Comparative Study Based on the Least Square Parameter Identification Method for State of Charge Estimation of a LiFePO_4 Battery Pack Using Three Model-Based Algorithms for Electric Vehicles

Taimoor Zahid ^{1,2,3} and Weimin Li ^{1,2,3,*}

¹ Shenzhen Institutes of Advanced Technology, Chinese Academy of Sciences, Shenzhen 518055, China; taimoor.z@siat.ac.cn

² Shenzhen College of Advanced Technology, University of Chinese Academy of Sciences, Shenzhen 518055, China

³ Jining Institute of Advanced Technology, Chinese Academy of Sciences, Jining 272000, China

* Correspondence: wm.li@siat.ac.cn; Tel.: +86-159-1537-4149

Academic Editor: Izumi Taniguchi

Received: 13 June 2016; Accepted: 26 August 2016; Published: 8 September 2016

Abstract: Battery energy storage management for electric vehicles (EV) and hybrid EV is the most critical and enabling technology since the dawn of electric vehicle commercialization. A battery system is a complex electrochemical phenomenon whose performance degrades with age and the existence of varying material design. Moreover, it is very tedious and computationally very complex to monitor and control the internal state of a battery's electrochemical systems. For Thevenin battery model we established a state-space model which had the advantage of simplicity and could be easily implemented and then applied the least square method to identify the battery model parameters. However, accurate state of charge (SoC) estimation of a battery, which depends not only on the battery model but also on highly accurate and efficient algorithms, is considered one of the most vital and critical issue for the energy management and power distribution control of EV. In this paper three different estimation methods, i.e., extended Kalman filter (EKF), particle filter (PF) and unscented Kalman Filter (UKF), are presented to estimate the SoC of LiFePO_4 batteries for an electric vehicle. Battery's experimental data, current and voltage, are analyzed to identify the Thevenin equivalent model parameters. Using different open circuit voltages the SoC is estimated and compared with respect to the estimation accuracy and initialization error recovery. The experimental results showed that these online SoC estimation methods in combination with different open circuit voltage-state of charge (OCV-SoC) curves can effectively limit the error, thus guaranteeing the accuracy and robustness.

Keywords: battery management system; lithium ion batteries; state of charge (SoC) estimation; extended Kalman filter (EKF); unscented Kalman filter (UKF); particle filter (PF)

1. Introduction

A battery management system is an important component of an electric vehicle especially in pure electric vehicles (PEV) where the battery is the only source of power. The battery applications for electric vehicles (EV), hybrid electric vehicle (HEV) and areas where batteries can be used as a primary source of energy have been widespread over the past few years due to the transition of internal combustion engine (ICE)-based automobile industries to EVs and HEVs [1]. Use of renewable electricity resources in EVs and HEVs plays a significant role in the transition towards sustainable transportation [2]. One of the major challenges faced by the current EV industry is the overall driving

range, which is much lower compared to the ICE vehicles. Adding to the problem is a lack of a battery management system that can estimate and predict the actual remaining power of a battery i.e., to predict the residual driving range. Therefore preventing EVs from running out of charge or leaving the passengers stranded is the main concern [3].

Thus, better control and management strategies for battery capacity are required in order to safeguard the performance and to extend the battery's useful life. In order to predict the residual range of the electric vehicle, one of the parameters directly involved in its calculation is state of charge (SoC). SoC describes the battery's remaining capacity status and is critically important for accurate measurement of EV battery state. SoC will give drivers an indication of available runtime and will also help to avoid some detrimental situations like overcharging or over-discharging which might reduce the useful lifespan of a power battery [4]. Therefore, there is a need for a battery that has high energy density, has a long service life and, most of all, is environmental friendly. Automotive industry nowadays considers Li-ion batteries as the preferred choice over the conventional batteries like Ni-MH, Mi-Cd and lead acid batteries due to its high single cell voltage, high energy density and long service life [4,5]. As opposed to the conventional methods for measuring the remaining gas or fuel in a car, SoC cannot be measured directly with physical sensors because of the battery's strong non-linear and time-variable system.

Several methods for estimating or measuring SoC have been proposed and reported [6–12]. Each method has its own pros and cons. SoC estimation methods can mainly be divided into two main categories. The first category includes non-model based techniques that are based on the type of measured or estimated input variable. The discharge test, open circuit voltage (OCV) and ampere hour counting methods all fall under this category. The discharge test method is very time consuming and viable only under laboratory conditions though it is one of the most reliable methods. Contrary to the discharge test method, the OCV-based SoC estimation method is a promising technique that obtains SoC from the battery's OCV-SoC relationship [2]. The second category deals with different kinds of battery models in combination with several adaptive control algorithms.

Battery models can also be further classified into three main categories i.e., (1) a physical model that is designed for a specific battery factor (e.g., temperature model [13] and cycle life model [14]). However, one specific factor cannot describe the functioning and operation of the whole battery; (2) an electro-chemical model that captures the significant electrochemical processes of a battery through a complex mathematical equation and as a consequence makes the state estimation process difficult [4,15]; (3) an equivalent circuit model (ECM) captures the electrochemical physics of a battery using only electrical components, and generally includes an n th order resistor-capacitor (RC) circuit with a series impedance factor, making it easy to incorporate into the system model of an electric vehicle with more precision and lower computational cost. However, according to [16] higher n th order RC circuit adds more non-linearity to the model, resulting in a more complex ECM.

Several adaptive control algorithms in combination with these battery models are used to estimate the states of a lithium ion battery. Different variants of Kalman filtering techniques are mostly used to estimate the SoC based on different battery models. The extended Kalman filter (EKF) was first used to estimate the SoC by Plett [5] and Xiong et al. [17–19] further improved it. However, Plett [20] came up with unscented Kalman filter (UKF) idea to overcome the drawbacks of EKF i.e., the derivation of Jacobian matrix is very trivial making it highly unstable during linearization. However for systems with high non-linearity or with a non-Gaussian model the overall estimation performance of the Kalman filter family decreases drastically. Therefore, a particle filter (PF) as an alternative solution has been presented in order to cope with the highly non-linear/non-Gaussian models. PF is a probability-based estimator that can be utilized for SoC estimation dealing with both the Gaussian and non-Gaussian distributed noise models. PF utilizes the particles (weighted random samples) to approximate the posterior distribution sampled by Monte-Carlo methods [21].

Besides system filtering theory, several other machine learning algorithms have been reported for SoC estimation [22–25] such as artificial neural networks (ANN), fuzzy logic based estimation and

many others. These estimation methods offer good performance but are computationally intensive and may require complex processors that are too expensive to be used in a real-time automotive energy management system. Support vector machine (SVM)-based regression offers an alternative method for SoC estimation. Using the principle of Vapnik-Chervonenkis (VC) dimensional statistical learning theory (SLT) and structural risk minimization theory, SVM builds an optimized network structure with the right balance between the empirical error and VC confidence interval. Thus, it achieves a better generalization performance than ANN [26]. However, the disadvantage is that they are dependent on the quality and quantity of the training data, which makes them computationally very expensive.

This paper adopts the least square method to identify the parameters of the lithium ion equivalent battery model and estimates SoC based on EKF, PF and UKF algorithms. The remainder of the paper is organized as follows. Section 2 discusses the battery model selected for the experiment while Section 3 briefly discusses the use of EKF, the application of Sequential Monte Carlo (SMO), i.e., PF and UKF, for Li ion battery SoC estimation based on the current integral method and the open-circuit voltage method, followed by the results and conclusion in Sections 4 and 5, respectively.

2. Battery Modeling

A battery model describes the relationship between the battery factors and its running characteristics. There are a lot of definitions found in the literature for SoC. In this paper, we will use the following definition: the SoC of a battery is the ratio of the full capacity to the present maximum available capacity. According to the SoC definition [27] it can be represented by Equation (1):

$$S_t = S_0 - \frac{1}{Q_m} \int_0^t \eta i_t d\tau \quad (1)$$

where S_t is the present SoC; S_0 is the initial SoC value; i_t is the instantaneous load current (as assumed positive and negative for discharging and charging phase respectively) and η is the columbic efficiency, which is determined by the aging of the battery. In this paper we assume $\eta = 1$. Q_m is the rated columbic capacity that differ from the battery's rated capacity due to the aging effect. Figure 1 shows the open circuit voltage.

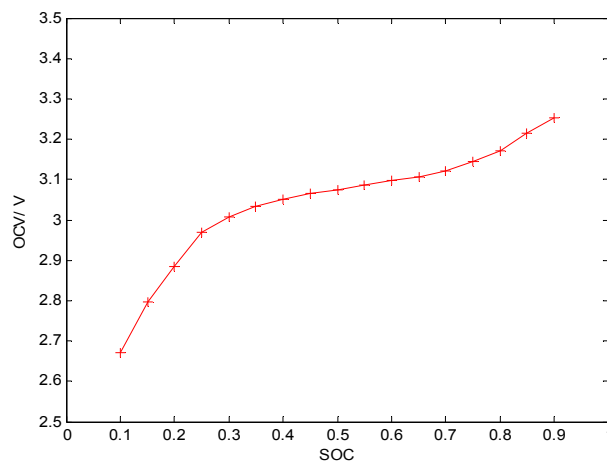


Figure 1. Discharge open circuit voltage state of charge (OCV-SoC) curve of LiFePO₄ battery at 25 °C, 10 A constant current [28,29].

As the algorithm will be implemented into a digital system, transforming Equation (1) into a discrete form gives Equation (2):

$$S_n = S_{n-1} - \frac{i_n \Delta n}{Q_m} \quad (2)$$

where n is the sampling step and Δn is the sampling period.

2.1. Battery Model

An ECM for Li ion battery with one OCV source and a parallel RC network was selected as shown in Figure 2.

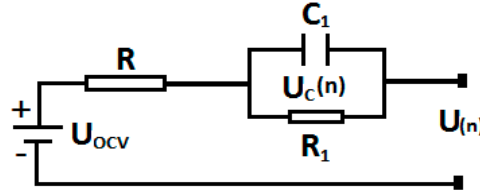


Figure 2. Battery equivalent circuit model (ECM).

The $U(n)$ source, parameterized as a non-linear function of the battery SoC and the OCV, is to describe the open circuit voltage characteristic at different SoC. Time-dependent polarization and diffusion effects of the cell are represented by the parallel ladder.

The state space equation of the battery circuit is presented in Equations (3) and (4).

$$\begin{bmatrix} U_c(n+1) \\ \text{SoC}(n+1) \end{bmatrix} = \begin{bmatrix} e^{(-\frac{\Delta T}{R_1 C_1})} & 0 \\ 0 & 1 \end{bmatrix} \begin{bmatrix} U_c(n) \\ \text{SoC}(n) \end{bmatrix} + \begin{bmatrix} R_1 \left(1 - e^{(-\frac{\Delta T}{R_1 C_1})}\right) \\ -\frac{\alpha \Delta T}{Q_m} \end{bmatrix} I_i(n) + \begin{bmatrix} r_n \\ v_n \end{bmatrix} \quad (3)$$

$$U(n) = F(\text{SoC}(n)) - U_c(n) - I_i(n) R_1 + R(n) \quad (4)$$

In the above model, $R_1 C_1$ is the time constant of the RC network. T is the sampling time and $U_{ocv} = F(\text{SoC}(n))$. r_n and v_n are assumed to be Gaussian noise.

2.2. Least Square Method

One of the most widely used method to find or estimate the numerical values of the parameters is least square method [30]. It can also be used to fit a function to a set of data and to characterize the statistical properties of the estimates. The principle of the least square method is as follows: a set of N pairs of observation $\{Y_i, X_i\}$ are used to find a function given the value of the dependent (Y) from the values of an independent variable (X). With one variable and a linear function, the prediction is given by Equation (5):

$$\hat{Y} = a + bX \quad (5)$$

In Equation 5, a and b are two free parameters which specify the slope and intercept of the regression line respectively. The least square method defines the estimate of these parameters as the value which minimizes the sum of squares between the measurements and the model. This amounts to minimizing the expression:

$$\varepsilon = \sum_i (Y_i - \hat{Y}_i)^2 = \sum_i [Y_i - (a + bX_i)]^2 \quad (6)$$

where ε stands for error which is the quantity to be minimized, and this is achieved using the standard technique property i.e., a quadratic formula reaches its minimum value when its derivatives vanishes. Taking the partial derivative of ε with respect to a and b and setting them to zero gives the following set of equations:

$$\frac{\partial \varepsilon}{\partial a} = 2Na + 2b \sum X_i - 2 \sum Y_i = 0 \quad (7)$$

$$\frac{\partial \varepsilon}{\partial b} = 2b \sum X_i^2 Na + 2a \sum X_i - 2 \sum Y_i X_i = 0 \quad (8)$$

To identify the parameters of the battery pack listed in Table 1 during the discharging process, a constant current pulse is produced, which is constant for sometime, in order to identify the relevant parameters by varying the pulse current as shown in Figure 3.

Table 1. Identified battery model parameters.

Parameter	Value	Unit
τ	9	s
R	3	m Ω
R_1	3	m Ω
C_1	3000	F

In this experiment, we obtained the parameters of the Thevenin battery model shown in Figure 2 based on the least square method and the characteristic of the voltage response of the constant pulse-current discharge. Figure 3 is the voltage response process of a 20 A constant pulse-current discharge. The parameter identification process is as follows: when the pulse-current is removed, the bus current $I = 0$, and the terminal voltage of the battery becomes $U(n) = U_{ocv} + U_c(n)$ until the polarized capacitor discharges gradually $U_c(n) = 0$.

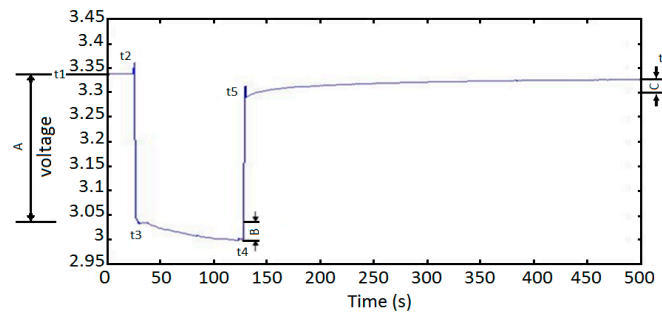


Figure 3. The voltage response process of the pulse-current discharge.

Phase C in Figure 3 shows the slow discharge reaction due to the capacitance C_1 of the RC circuit at the end of the discharge process until the voltage returns to normal. The zero input response of the RC circuit is $U'_c(n) = U_c(n) e^{(-n/\tau)}$ in which $\tau = R_1 C_1$ is the time constant. Apply the least square method to obtain τ .

$$\tau = R_1 C_1 = \frac{[\sum_{i=1}^m n_i]^2 - \sum_{i=1}^m n_i^2}{[m \sum_{i=1}^m n_i (\ln u_i)] - \sum_{i=1}^m n_i \sum_{i=1}^m (\ln u_i)} \quad (9)$$

Phase B in Figure 3 consists of two parts. One part is the voltage drop of the terminal voltage which is caused by the pulse-current discharge. The second part is the voltage drop of the RC circuit. Thus we can easily get the voltage drop of the RC circuit $U_c(n)$. The zero-state response of the RC circuit is $U_c(n) = IR_1 e^{-\frac{n}{\tau}}$. By applying the least square method again, we can get the parameters R_1 and C_1 .

$$R_1 = \frac{e[\frac{1}{m} \sum_{i=1}^m (\ln u_i) - \frac{\tau}{m} \sum_{i=1}^m n_i]}{I} \quad (10)$$

$$C_1 = \frac{\tau}{R_1} \quad (11)$$

The ohmic resistance parameter R is obtained from voltage drop difference in phase A of the response process shown in Figure 3.

$$R = \frac{(U_1 - U_2)}{I} \quad (12)$$

Thus all the parameters of the battery ECM are obtained.

3. Battery SoC Estimation Approach

3.1. Extended Kalman Filter

EKF is a non-linear version of the Kalman filter as the non-linear function is Taylor expanded and the high order terms are ignored. A brief summary of EKF is given below:

Summary of Conventional Non-Linear EKF	
Non-linear state-space model	
$\bar{\mathbf{X}}_{n+1} = F(\bar{\mathbf{X}}_n, U_n) + r_n$ $\bar{\mathbf{Y}}_{n+1} = G(\bar{\mathbf{X}}_n, U_n) + v_n$	
Definitions	
$F(\bar{\mathbf{X}}_n, U_n) \approx F(\hat{\mathbf{X}}_n, U_n) + \left. \frac{\partial F(\bar{\mathbf{X}}_n, U_n)}{\partial \bar{\mathbf{X}}_n} \right _{\bar{\mathbf{X}}_n = \hat{\mathbf{X}}_n} (\bar{\mathbf{X}}_n - \hat{\mathbf{X}}_n)$ $G(\bar{\mathbf{X}}_n, U_n) \approx G(\hat{\mathbf{X}}_n, U_n) + \left. \frac{\partial G(\bar{\mathbf{X}}_n, U_n)}{\partial \bar{\mathbf{X}}_n} \right _{\bar{\mathbf{X}}_n = \hat{\mathbf{X}}_n} (\bar{\mathbf{X}}_n - \hat{\mathbf{X}}_n)$ $\hat{\mathbf{A}}_n = \left. \frac{\partial F(\bar{\mathbf{X}}_n, U_n)}{\partial \bar{\mathbf{X}}_n} \right _{\bar{\mathbf{X}}_n = \hat{\mathbf{X}}_n}^+, \hat{\mathbf{C}}_n = \left. \frac{\partial F(\bar{\mathbf{X}}_n, U_n)}{\partial \bar{\mathbf{X}}_n} \right _{\bar{\mathbf{X}}_n = \hat{\mathbf{X}}_n}^-$	
Initialization	
$\hat{\mathbf{X}}_0^+ = E[\bar{\mathbf{X}}_0]$ $\Sigma_{\bar{\mathbf{X}},0}^+ = E[(\bar{\mathbf{X}}_0 - \hat{\mathbf{X}}_0^+)(\bar{\mathbf{X}}_0 - \hat{\mathbf{X}}_0^+)^T]$	
Computation	
State estimate time: $\hat{\mathbf{X}}_n^- = F(\hat{\mathbf{X}}_{n-1}^+, U_{n-1})$ Error covariance time: $\Sigma_{\bar{\mathbf{X}},n}^- = \hat{\mathbf{A}}_{n-1} \Sigma_{\bar{\mathbf{X}},n-1}^+ \hat{\mathbf{A}}_{n-1}^T + \Sigma_w$ Kalman gain matrix: $K_n = \Sigma_{\bar{\mathbf{X}},n}^- \hat{\mathbf{C}}_n^T [\hat{\mathbf{C}}_n \Sigma_{\bar{\mathbf{X}},n}^- \hat{\mathbf{C}}_n^T + \Sigma_v]^{-1}$ State estimate measurement: $\hat{\mathbf{X}}_n^+ = \hat{\mathbf{X}}_n^- + K_n [\bar{\mathbf{Y}}_n - G(\hat{\mathbf{X}}_n^-, U_n)]$ Error covariance measurement: $\Sigma_{\bar{\mathbf{X}},n}^+ = (I - K_n \hat{\mathbf{C}}_n) \Sigma_{\bar{\mathbf{X}},n}^-$	

3.2. Unscented Kalman Filter

For non-linear systems, UKF uses numeric approximations rather than analytic approximations. First UKF chooses a set of sigma (σ) points then the mean and covariance of these points are used to match the priori random variable's mean and covariance in every estimation step. A weighting constant is assigned to each σ point and the overall sum of all the weighting constants is equal to 1. As a result we get a set of transformed points after passing all the σ points through a non-linear function. Finally, the mean and covariance of the transformed points are used to update the posteriori mean and covariance. One of the major differences between UKF and EKF is the σ point calculation.

The process model is described in Equation (13):

$$\bar{\mathbf{X}}_n = F(\bar{\mathbf{X}}_{n-1}, u_{n-1}, \mathbf{r}_{n-1}, n-1) \quad (13)$$

The state vector $\bar{\mathbf{X}}_n = [U_c \quad \text{SoC}]^T$, is a discrete process. u_n and $\mathbf{r}_n = [r_{UC} \quad r_{\text{SoC}}]^T$ are the control vectors and process noise respectively.

The observation model is described in Equation (14):

$$\bar{\mathbf{Y}}_{n+1} = G(\bar{\mathbf{X}}_n, u_n, v_n, n) \quad (14)$$

Here v_n is the measurement noise. Including the noise in Equation (14) gives us the new state vector presented in Equation (15).

$$\bar{X} = [U_c, \text{SoC}, r_{UC}, r_{SoC}, r_U]^T \quad (15)$$

The process noise r_{UC} , r_{SoC} and measurement noise r_U are Gaussian random processes with zero mean.

- Choose σ points

The state vector \bar{X} has dimension $M = 5$, mean \bar{x} and covariance \bar{P}_X , then $p + 1 = 2M + 1 = 11$. σ points with their weight factors are generated using Equation (16):

$$\begin{cases} \chi_{s0} = \bar{x}j = 0 \\ \chi_{sj} = \bar{x} + \left(\sqrt{(M + \lambda) \bar{P}_X} \right)_i j = 1, 2, \dots, M \\ \chi_{sj} = \bar{x} + \left(\sqrt{(M + \lambda) \bar{P}_X} \right)_{i-M} j = M + 1, \dots, 2M \\ w_0^{(sm)} = \frac{\lambda}{M + \lambda} \\ w_0^{(sc)} = \frac{\lambda}{M + \lambda} + 1 - w^2 + \beta \\ w_j^{(sm)} = w_j^{(sc)} = \frac{1}{2(M + \lambda)} j = 1, 2, \dots, 2M \end{cases} \quad (16)$$

$\left(\sqrt{(M + \lambda) \bar{P}_X} \right)_j$ is the i th column of the matrix square root of $(M + \lambda) \bar{P}_X$. $w^{(sm)}$ is the weighting and $w_0^{(sc)}$ is the weighting constant of σ point mean and σ point covariance respectively. They are defined as $\bar{X} = \sum_{j=0}^{2M} w_j^{(sm)} \chi_{sj}$, $\bar{P}_X = \sum_{j=0}^{2M} w_j^{(sc)} (\chi_{sj} - \bar{X})(\chi_{sj} - \bar{X})^T$. λ is a scaling factor defined as $\lambda = w^2 (M + n) - M$. The spread of the σ points is represented by w . β incorporates prior information and $\beta = 2$ is the optimal value for the Gaussian distributions. n is either 0 or $3 - M$.

- Initialization step:

$$\bar{X}_0^+ = E[\bar{x}_0] = [U_c, \text{SoC}, 0, 0, 0]^T \quad (17)$$

- State estimate time update step:

$$\bar{P}_0^+ = E \left[(\chi_{s0} - \bar{X}_0^+) (\chi_{s0} - \bar{X}_0^+)^T \right] = \text{diag}(T, Q, R) \quad (18)$$

T , Q and R are the variance matrix of the primitive state variable $\bar{X}_n = [U_c, \text{SoC}]^T$, process noise $r_n = [r_{UC}, r_{SoC}]^T$ and the measurement noise v respectively.

- State estimate time update

Rewrite the σ points through Equation (3). We will get $2M + 1$ σ points $\chi_{s_{n,j}}^-$, $i = 0, 1, \dots, 2M$. The mean and covariance of the state vector can be calculated using Equations (19) and (20):

$$\bar{X}_n^- = \sum_{j=0}^{2M} w_j^{(sm)} \chi_{s_{n,j}}^- \quad (19)$$

$$\bar{P}_{X,n}^- = \sum_{j=0}^{2M} w_j^{(sc)} \chi_{s_{n,j}}^- \left(\chi_{s_{n,j}}^- - \bar{X}_n^- \right) \left(\chi_{s_{n,j}}^- - \bar{X}_n^- \right)^T \quad (20)$$

- Output estimate

Propagating the σ points through the observation function given in Equation (4) results in Equation (21):

$$\bar{Y}_{n,j} = G \left(\chi_{n,j}^{\bar{-}}, u_n, \chi_{n,j}^{v,+}, n \right) \quad (21)$$

Then, using Equations (22) and (23) to calculate the mean and covariance of the estimated output:

$$\hat{Y}_n = \sum_{j=0}^{2M} w_j^{(sm)} \bar{Y}_{n,j} \quad (22)$$

$$\bar{P}_{\bar{Y},n} = \sum_{j=0}^{2M} w_j^{(sc)} (\bar{Y}_{n,j} - \hat{Y}_n) (\bar{Y}_{n,j} - \hat{Y}_n)^T \quad (23)$$

- Estimator Kalman gain matrix

In order to calculate the Kalman gain, the covariance matrix must be calculated prior to it being used in Equation (24):

$$\bar{P}_{\bar{X}\bar{Y},n} = \sum_{j=0}^{2M} w_j^{(sc)} \bar{Y}_{n,j} \left(\chi_{n,j}^{s,-} - \bar{X}_n \right) (\bar{Y}_{n,j} - \hat{Y}_n)^T \quad (24)$$

Then:

$$K_n = \bar{P}_{\bar{X}\bar{Y},n} / \bar{P}_{\bar{Y},n} \quad (25)$$

- State estimate measurement update

Finally, update the state vector using Equations (26) and (27):

$$\bar{X}_n^+ = \bar{X}_n^- + K_n (\bar{Y}_n - \hat{Y}_n) \quad (26)$$

$$\bar{P}_{\bar{X},n}^+ = \bar{P}_{\bar{X},n}^- - K_n \bar{P}_{\bar{Y},n} K_n^T \quad (27)$$

3.3. Particle Filter as a Sequential Monte Carlo Method

For complex battery models with strong non-linearity PF can be utilized to perform the SoC estimation. PF is a Monte Carlo method (SMC) that integrates the Bayesian learning methods with sequential importance sampling (SIS) and re-sampling. PF approximates the posterior by a set of particles associated with weights without any assumption of its form. In Monte Carlo simulation for state estimation, the given state X_n will be estimated with the observation Y_n . The given equation can be utilized to approximate the posterior using Equation (28):

$$p(\bar{X}_{0:n} | \bar{Y}_{1:n}) = \frac{1}{K} \sum_{i=1}^K \delta_{\bar{X}_{0:n}^i} d\bar{X}_{0:n} \quad (28)$$

$\bar{X}_{0:n}^i$ ($i = 1, 2, \dots, K$) are the random samples drawn from the posterior distribution and estimate Equation (29) can be utilized to approximate any expectations:

$$\overline{E(\bar{Y}_n(\bar{X}_{0:n}))} = \frac{1}{K} \sum_{i=1}^K G_n(\bar{X}_{0:n}^i) \quad (29)$$

Without directly sampling from the posterior density function we can sample from the proposal distribution $q(\bar{X}_{0:n} | Y_{1:n})$ [15], and we can derive Equation (30):

$$\overline{E(\bar{Y}_n(\bar{X}_{0:n}))} = \frac{1}{K} \sum_{i=1}^K G_n(\bar{X}_{0:n}^i) w_n(\bar{X}_{0:n}^i) \quad (30)$$

Here w is the normalized importance weight. Normalize the weight for each particle (i.e., sum to total that equals 1) using Equations (31) and (32):

$$w_n(\bar{\mathbf{X}}_{0:n}^i) = \frac{p(\bar{\mathbf{X}}_{0:n}|\bar{\mathbf{Y}}_{1:n}) p(\bar{\mathbf{X}}_{0:n})}{q(\bar{\mathbf{X}}_{0:n}|\bar{\mathbf{Y}}_{1:n})} \quad (31)$$

$$w_n^i = \frac{w_n^i}{\sum_{j=1}^K w_n^j} \quad (32)$$

Hence we can approximate the empirical estimate Equation (28) as the following posterior density function in Equation (33):

$$p(\bar{\mathbf{X}}_{0:n}|\bar{\mathbf{Y}}_{1:n}) = \frac{1}{K} \sum_{i=1}^K w_n^i \delta_{\bar{\mathbf{X}}_{0:n}^i} d\bar{\mathbf{X}}_{0:n} \quad (33)$$

Assuming the Markov process for the state we get Equation (34):

$$w_n = w_{n-1} \frac{p(\bar{\mathbf{X}}_{0:n}|\bar{\mathbf{Y}}_{1:n}) p(\bar{\mathbf{X}}_{0:n})}{q(\bar{\mathbf{X}}_{0:n}|\bar{\mathbf{Y}}_{1:n})} \quad (34)$$

Hence the optimal choice for the proposal distribution is presented in Equation (35):

$$q(\bar{\mathbf{X}}_n|\bar{\mathbf{X}}_{n-1}, \bar{\mathbf{Y}}_{1:n}) = p(\bar{\mathbf{X}}_n|\bar{\mathbf{Y}}_{n-1}) \quad (35)$$

PF for SoC Estimation

For SoC estimation PF works in two simple steps, i.e., predict and update. According to the previous discussion about PF review, PF-based Li ion battery SoC estimation algorithm is discussed below:

- Initialization.

Select the total number of particles L and generate the initial particles by using Equation (36):

$$\bar{\mathbf{X}}_0^i = \bar{\mathbf{X}}_0 + N(\bar{\mathbf{X}}_0, \sigma^2) \quad i = (1, 2, 3, \dots, L) \quad (36)$$

$N(\bar{\mathbf{X}}_0, \sigma^2)$ is the Gaussian distribution where $\bar{\mathbf{X}}_0$ is the initial guess and σ^2 is the error covariance.

- State prediction.

Propagate the particles $\bar{\mathbf{X}}_{n-1}^i$ using the system process equation $\bar{\mathbf{X}}_0^i = F(\bar{\mathbf{X}}_{n-1}, V_{n-1}) + N(\bar{\mathbf{X}}_0, \sigma^2)$ to predict a new set of particles.

- Weight calculation and normalization step (importance sampling).

After calculating the particles maximum likelihood using Equation (37), generate the weights according to Equation (38) and then normalize the weights (Equation (39):

$$m_i = \frac{\exp\left(-\frac{1}{2\sqrt{r}}\left(\bar{\mathbf{Y}}_n - \left(\bar{\mathbf{X}}_n^i, V_n\right)\right)^2\right)}{\sqrt{2\pi r}} \quad (37)$$

$$w_n^i = w_{n-1}^i m_i \quad (38)$$

$$w_n^i = \frac{w_n^i}{\sum_{j=1}^L w_n^j} \quad (39)$$

- Re-sampling step.

After normalization of the weights, generate random and uniform samples with a residual re-sampling technique.

- Determine output estimate using Equation (40):

$$\bar{X}_n = \frac{1}{L} \sum_{i=1}^L w_n^i \bar{X}_n^i \quad (40)$$

\bar{X}_n is the estimated SoC using PF. Repeat Steps 2–5 for all $n = 1, 2, \dots$

4. Experimental Results and Discussion

To validate the performance of EKF, UKF and PF, we used Shenzhen top band LiFePO₄ “3470160” cells (Shenzhen TOPBAND, Guangdong, China). The capacity of each single cell is 20 Ah, 3.2 V. The current and voltage information of the battery pack were recorded using a Digatron battery testing system (BTS) that has the capability to perform charge/discharge of multiple cells simultaneously to obtain charge-discharge capacity and energy. A host computer running the battery testing software recorded all the battery data including voltage, current, Ampere-hour (Ah) and temperature etc. Overall voltage and current sensors error were between 0.1% and 0.5% respectively. For noise cancelation, BTSs have a low pass filtering function. Battery SoC experimental data with the given sampled current and voltage was obtained by BTS management module’s designed algorithm shown in Figure 4.

In practical situation a battery’s actual capacity is limited within the range of 90%–10% to protect it from any damage. 17 points from the voltage plateau area (from 2.6 V to 3.3 V) were chosen in order to get the constant current discharge curve of LiFePO₄ at 25 °C shown in Figure 1.

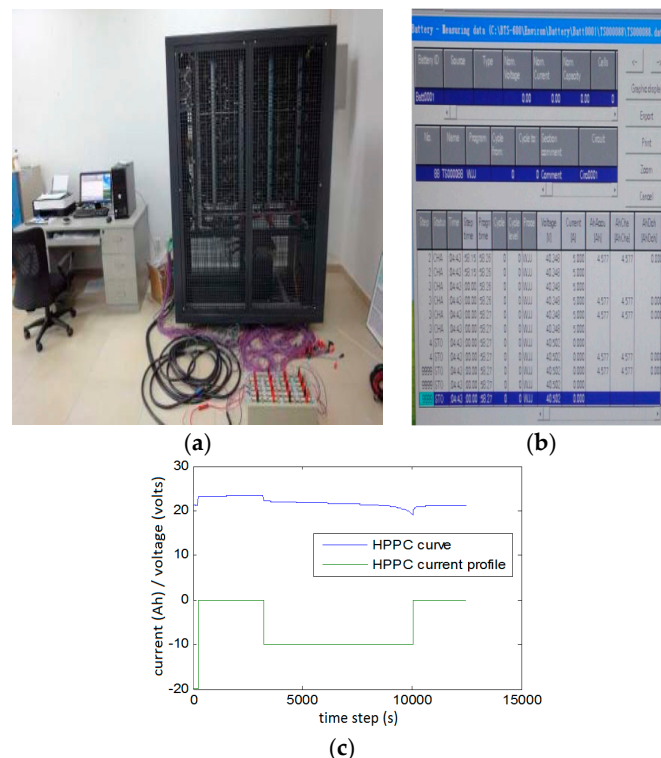


Figure 4. (a) Battery test bench (Digatron + batteries); (b) data acquisition system interface; and (c) hybrid pulse power characterization (HPPC) profile.

From Figure 1 it can be seen that the relationship between SoC and OCV is intrinsically non-linear. In order to describe this non-linear behavior we used 4 different kinds of OCV function [31–33] to fit

the OCV-SoC curve for SoC estimation given in Table 2. The goodness-of-fit evaluation factors sum of squared error (SSE), R^2 , adjusted R^2 and root mean square error (RMSE) are derived for each OCV function selected for SoC estimation. Table 3 shows the experimental data for the identification of the parameters. All the parameters (Table 4) were obtained from the OCV-SoC curve with their respective goodness of fit shown in Table 5.

Table 2. Candidate OCV functions.

No	Description
1	$U_{ocv} = a_0 + \frac{a_1}{s} + a_2s + a_3\ln(s) + a_4\ln(1-s)$
2	$U_{ocv} = a_0 + \frac{a_1}{s} + a_2s^2 + a_3e^{-a_4(1+s)}$
3	$U_{ocv} = a_0s^3 + a_1s^2 + a_2s + a_3$
4	$U_{ocv} = a_0s^4 + a_1s^3 + a_2s^2 + a_3s + a_4$

In Table 2, “ s ” represents the SoC of the battery and “ a_1 – a_4 ” is the coefficient obtained from the OCV-SoC curves.

Table 3. Experimental data for identification of parameters for $U_{ocv} = F(\text{SoC}(n))$.

SoC	0.1	0.15	0.2	0.25	0.3	0.35	0.4	0.45	0.5	0.55	0.6	0.65	0.7	0.75	0.8	0.85	0.9
Uocv	2.67	2.79	2.88	2.96	3	3.03	3.05	3.06	3.07	3.08	3.09	3.1	3.12	3.14	3.17	3.21	3.25

Table 4. Candidate OCV functions parameters.

OCV Function	a_0	a_1	a_2	a_3	a_4
1	3.817	0.001086	−1.152	0.4646	−0.2309
2	1.877	−0.02616	−3.935	0.1507	−1.799
3	3.622	−6.122	3.552	2.387	−
4	−3.354	10.33	−10.64	4.718	2.296

Table 5. Goodness of fit.

OCV Function	SSE *	R^2 **	Adjusted R^2	RMSE ***
1	0.0009759	0.9972	0.9962	0.009018
2	0.0006527	0.9981	0.9975	0.007375
3	0.001302	0.9962	0.9954	0.01001
4	0.0002387	0.9993	0.9991	0.00446

* SSE: sum of squared error; ** R^2 : the coefficient of determination; *** RMSE: root mean square error.

Artificial Gaussian noise is added to the current (around 2% of the full range) in order to better evaluate the robustness of the SoC estimator in an environment close to a realistic automotive environment. Figures 5 and 6 show the battery SoC estimation using the EKF, UKF and PF. During the experiments, 200 particles were chosen, but it was observed that the PF algorithm showed the same error even with 1000–2000 particles at the cost of high computational time.

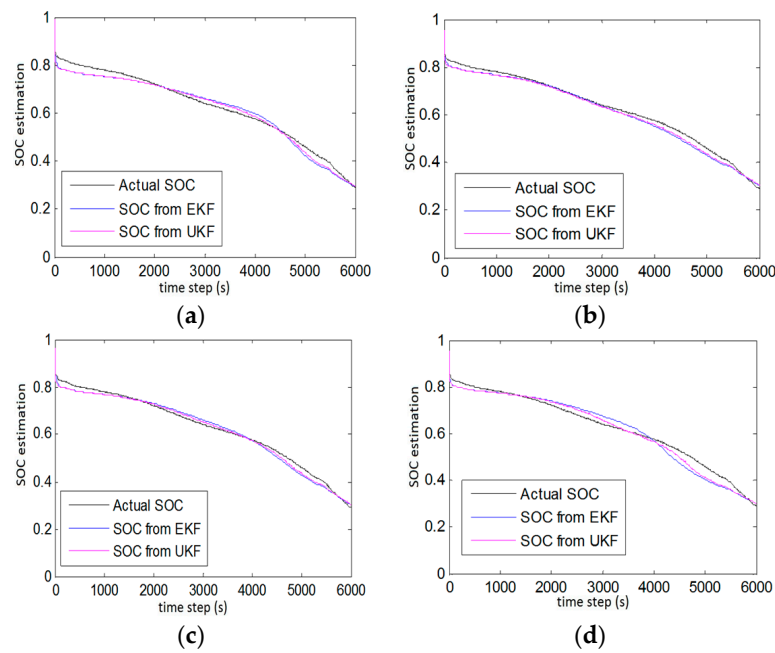


Figure 5. SoC estimation using unscented Kalman filter (UKF) and extended Kalman filter (EKF) using: (a) OCV Function 2; (b) OCV Function 4; (c) OCV Function 3; and (d) OCV Function 1.

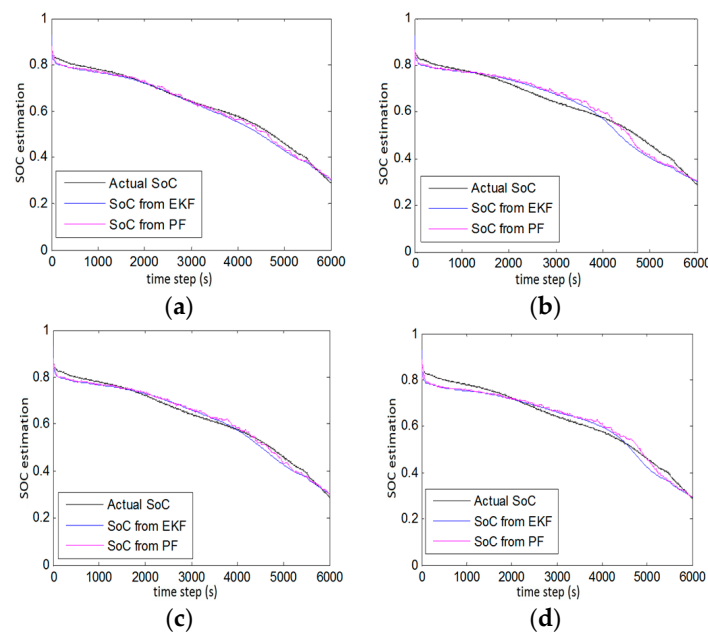


Figure 6. SoC estimation using particle filter (PF) and EKF using: (a) OCV Function 4; (b) OCV Function 1; (c) OCV Function 3; and (d) OCV Function 2.

Choosing the right OCV function is the key to better estimating the SoC of the battery. Good estimation results were obtained when a logarithmic, exponential model with a polynomial exponent and high order polynomial functions were used. The overall performance of the logarithmic and high order polynomial functions is much better than that of exponential model with a polynomial OCV function (Figure 7).

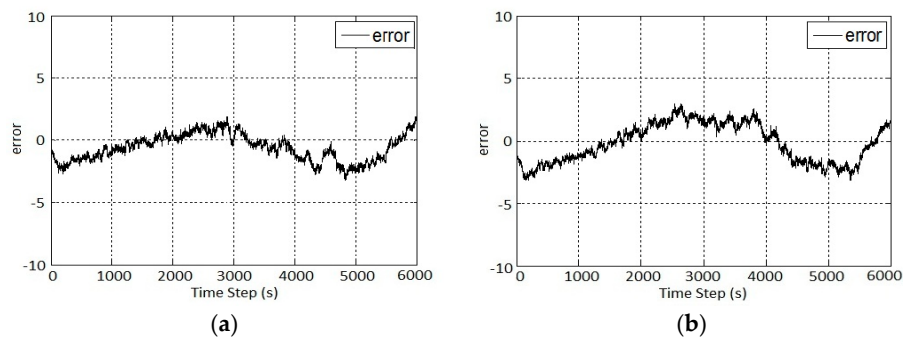


Figure 7. EKF and PF Error: (a) OCV Function 2; and (b) OCV Function 1.

The higher the order of the polynomial function the better it fits as can be seen in Figure 5b,c and Figure 6a,c where a 4th order polynomial function produced better estimation results than a 3rd order polynomial function (Table 5). However, the logarithmic function showed good estimation results with PF, but overall, UKF not only better tracked the actual SoC but also produced good estimation results.

During the experiments it was noticed that all the SoC estimation methods, i.e., EKF, UKF and PF, exhibited a large error when the SoC is between 65% and 45%. The smoothness of the OCV-SoC curve is responsible for this estimation error.

In Figure 8a, it can be seen that when incorrect SoC is given, i.e., initial SoC = 0.1, PF was affected the most. Although it started tracking the actual SoC later, it took some time to recover the initialization error. However, UKF proved better than EKF though they also suffered from initialization error recovery as shown in Figure 8b. Although both EKF and UKF were faster in terms of initialization error recovery but PF outperformed EKF when the battery model was affected by Gaussian noise or a higher order battery model is used which will add more non-linearity to the overall system shown in Figure 9.

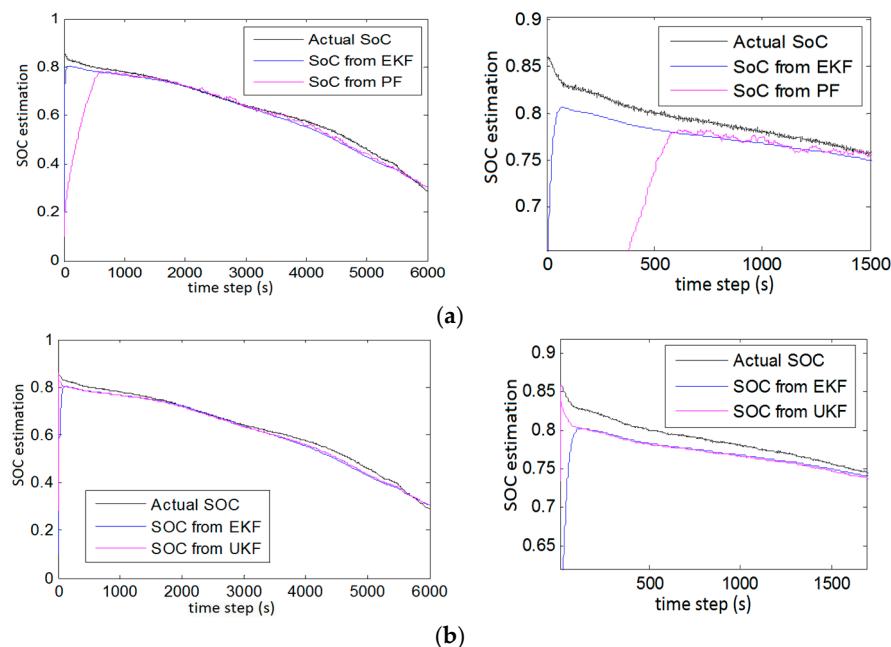


Figure 8. Initialization error recovery test using OCV Function 4: (a) EKF and PF; (b) EKF and UKF.

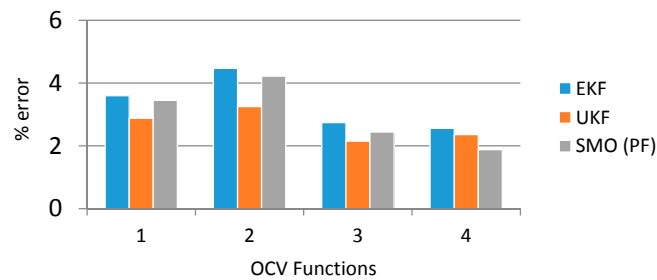


Figure 9. EKF, UKF and Sequential Monte Carlo (SMO (PF)) error comparison.

This experiment showed that both methods can be used as an alternative to the traditional EKF method in overcoming its weakness, i.e., higher order battery models, initialization error recovery and low accuracy. The overall percentage error is listed in Table 6.

Table 6. EKF, UKF and PF error comparison.

OCV Function	EKF (%)	UKF (%)	PF (%)
1	3.60	2.88	3.45
2	4.47	3.25	4.22
3	2.74	2.15	2.44
4	2.56	2.36	1.88

5. Conclusions

This paper presents a comparison between three different SoC estimation methods, i.e., EKF, UKF and PF, for a Li ion battery using four different OCV functions at 25 °C. LiFePO₄ was selected as the experimental battery and its model parameters were calculated using the least mean square method. PF was introduced in this paper as an alternate to EKF. SoC estimation with four different OCV functions was carried out. UKF in combination with an exponential model with a polynomial exponent performed better. Both EKF and UKF can overcome the initialization error recovery more rapidly than PF, and UKF proved to be more effective and accurate.

Acknowledgments: This work is supported by National Natural Science Foundation of China (Grant No. 61573337).

Author Contributions: Taimoor Zahid and Weimin Li conceived and designed the experiments, Taimoor Zahid performed the experiments and analyzed the data, Weimin Li contributed the experiment platform, Taimoor Zahid and Weimin Li wrote the paper.

Conflicts of Interest: The authors declare no conflict of interest.

References

1. Chang, W.-Y. State of charge estimation for LiFePO₄ battery using artificial neural network. *Int. Rev. Electr. Eng.* **2012**, *7*, 5874–5880.
2. Coleman, M.; Lee, C.K.; Zhu, C.; Hurley, W.G. State-of-charge determination from EMF voltage estimation: Using impedance, terminal voltage, and current for lead-acid and lithium-ion batteries. *IEEE Trans. Ind. Electron.* **2007**, *54*, 2550–2557. [[CrossRef](#)]
3. U.S. Department of Energy National Laboratory. Battery Test Manual for Plug-in Hybrid. Electric Vehicles, September 2010. Available online: <https://inldigitallibrary.inl.gov/sti/4655291.pdf> (accessed on 16 June 2016).
4. Chaturvedi, N.A.; Klein, R.; Christensen, J.; Ahmed, J.; Kojic, A. Algorithms for advanced battery-management systems. *IEEE Control. Syst.* **2010**, *30*, 49–68. [[CrossRef](#)]
5. Plett, G.L. Extended Kalman filtering for battery management systems of LiPB-based HEV battery packs: Part 3. State and parameter estimation. *J. Power Sources* **2004**, *134*, 277–292. [[CrossRef](#)]
6. Chiang, Y.-H.; Sean, W.-Y.; Ke, J.-C. Online estimation of internal resistance and open-circuit voltage of lithium-ion batteries in electric vehicles. *J. Power Sources* **2011**, *196*, 3921–3932. [[CrossRef](#)]

7. He, H.; Zhang, X.; Xiong, R.; Xu, Y.; Guo, H. Online model-based estimation of state-of-charge and open-circuit voltage of lithium-ion batteries in electric vehicles. *Energy* **2012**, *39*, 310–318. [[CrossRef](#)]
8. Hua, Y.; Xu, M.; Li, M.; Ma, C.; Zhao, C. Estimation of state of charge for two types of Lithium-Ion batteries by non-linear predictive filter for electric vehicles. *Energies* **2015**, *8*, 3556–3577. [[CrossRef](#)]
9. Ng, K.S.; Moo, C.-S.; Chen, Y.-P.; Hsieh, Y.-C. Enhanced coulomb counting method for estimating state-of-charge and state-of-health of lithium-ion batteries. *Appl. Energy* **2009**, *86*, 1506–1511. [[CrossRef](#)]
10. Schweiger, H.-G.; Obeidi, O.; Komesker, O.; Raschke, A.; Schiemann, M.; Zehner, C.; Gehnen, M.; Keller, M.; Birke, P. Comparison of several methods for determining the internal resistance of lithium ion cells. *Sensors* **2010**, *10*, 5604–5625. [[CrossRef](#)] [[PubMed](#)]
11. Yan, J.; Xu, G.; Qian, H.; Xu, Y. Robust state of charge estimation for hybrid electric vehicles: Framework and algorithms. *Energies* **2010**, *3*, 1654–1672. [[CrossRef](#)]
12. Zhang, H.; Zhao, L.; Chen, Y. A lossy counting-based state of charge estimation method and its application to electric vehicles. *Energies* **2015**, *8*, 13811–13828. [[CrossRef](#)]
13. Quanshi, C.; Chengtao, L. Summarization of studies on performance models of batteries for electric vehicle. *Automob. Technol.* **2005**, *3*, 1–5.
14. Ning, G.; White, R.E.; Popov, B.N. A generalized cycle life model of rechargeable Li-ion batteries. *Electrochim. Acta* **2006**, *51*, 2012–2022. [[CrossRef](#)]
15. Xu, J.; Mi, C.C.; Cao, B.; Cao, J. A new method to estimate the state of charge of lithium-ion batteries based on the battery impedance model. *J. Power Sources* **2013**, *233*, 277–284. [[CrossRef](#)]
16. Einhorn, M.; Conte, F.V.; Kral, C.; Fleig, J. Comparison, selection, and parameterization of electrical battery models for automotive applications. *IEEE Trans. Power Electron.* **2013**, *28*, 1429–1437. [[CrossRef](#)]
17. Xiong, R.; Gong, X.; Mi, C.C.; Sun, F. A robust state-of-charge estimator for multiple types of lithium-ion batteries using adaptive extended Kalman filter. *J. Power Sources* **2013**, *243*, 805–816. [[CrossRef](#)]
18. Xiong, R.; Sun, F.; Chen, Z.; He, H. A data-driven multi-scale extended Kalman filtering based parameter and state estimation approach of lithium-ion olymer battery in electric vehicles. *Appl. Energy* **2014**, *113*, 463–476. [[CrossRef](#)]
19. Xiong, R.; Sun, F.; He, H.; Nguyen, T.D. A data-driven adaptive state of charge and power capability joint estimator of lithium-ion polymer battery used in electric vehicles. *Energy* **2013**, *63*, 295–308. [[CrossRef](#)]
20. Plett, G.L. Sigma-point Kalman filtering for battery management systems of LiPB-based HEV battery packs: Part 1: Introduction and state estimation. *J. Power Sources* **2006**, *161*, 1356–1368. [[CrossRef](#)]
21. Gao, M.; Liu, Y.; He, Z. Battery state of charge online estimation based on particle filter. In Proceedings of the 2011 4th International Congress on Image and Signal Processing (CISP), Shanghai, China, 15–17 October 2011; pp. 2233–2236.
22. Feng, X.; Li, J.; Ouyang, M.; Lu, L.; Li, J.; He, X. Using probability density function to evaluate the state of health of lithium-ion batteries. *J. Power Sources* **2013**, *232*, 209–218. [[CrossRef](#)]
23. Han, S.-S.; Chen, W.-Z. The algorithm of dynamic battery SoC based on mamdani fuzzy reasoning. In Proceedings of the Fifth International Conference on Fuzzy Systems and Knowledge Discovery (FSKD'08), Jinan, China, 18–20 October 2008; pp. 439–443.
24. Linda, O.; William, E.J.; Huff, M.; Manic, M.; Gupta, V.; Nance, J.; Hess, H.; Rufus, F.; Thakker, A.; Govar, J. Intelligent neural network implementation for SOCI development of Li/CFx batteries. In Proceedings of the 2nd International Symposium on Resilient Control Systems (ISRCS'09), Idaho Falls, ID, USA, 11–13 August 2009; pp. 57–62.
25. Zenati, A.; Desprez, P.; Razik, H. Estimation of the SoC and the SOH of Li-ion Batteries, by combining Impedance Measurements with the Fuzzy Logic Inference. In Proceedings of the 36th Annual Conference on IEEE Industrial Electronics Society (IECON 2010), Glendale, AZ, USA, 7–10 November 2010; pp. 1773–1778.
26. Hansen, T.; Wang, C.-J. Support vector based battery state of charge estimator. *J. Power Sources* **2005**, *141*, 351–358. [[CrossRef](#)]
27. Hariharan, K.S.; Kumar, V.S. A non-linear equivalent circuit model for lithium ion cells. *J. Power Sources* **2013**, *222*, 210–217. [[CrossRef](#)]
28. Zhao, L.; Xu, G.; Li, W.; Taimoor, Z.; Song, Z. LiFePO₄ battery pack capacity estimation for electric vehicles based on unscented Kalman filter. In Proceedings of the 2013 IEEE International Conference on Information and Automation (ICIA), Yinchuan, China, 26–28 August 2013; pp. 301–305.

29. Zahid, T.; Xu, G.; Li, W.; Zhao, L.; Xu, K. Performance analysis of particle filter for SoC estimation of LiFePO₄ battery pack for electric vehicles. In Proceedings of the 2014 IEEE International Conference on Information and Automation (ICIA), Hulun Buir, China, 28–30 July 2014; pp. 1061–1065.
30. Abdi, H. The method of least squares. In *Encyclopedia of Measurement and Statistics*; SAGE Publications Inc.: Thousand Oaks, CA, USA, 2007.
31. Yu, Z.; Huai, R.; Xiao, L. State-of-charge estimation for lithium-ion batteries using a kalman filter based on local linearization. *Energies* **2015**, *8*, 7854–7873. [[CrossRef](#)]
32. Plett, G.L. Extended Kalman filtering for battery management systems of LiPB-based HEV battery packs: Part 2. Modeling and identification. *J. Power Sources* **2004**, *134*, 262–276. [[CrossRef](#)]
33. Tian, Y.; Chen, C.; Xia, B.; Sun, W.; Xu, Z.; Zheng, W. An adaptive gain non-linear observer for state of charge estimation of lithium-ion batteries in electric vehicles. *Energies* **2014**, *7*, 5995–6012. [[CrossRef](#)]



© 2016 by the authors; licensee MDPI, Basel, Switzerland. This article is an open access article distributed under the terms and conditions of the Creative Commons Attribution (CC-BY) license (<http://creativecommons.org/licenses/by/4.0/>).